Est. 1984

ORIENTAL JOURNAL OF CHEMISTRY
An International Open Access, Peer Reviewed Research Journal

www.orientjchem.org

ISSN: 0970-020 X
CODEN: OJCHEG
2023, Vol. 39, No.(6):
Pg. 1547-1555

Evaluation of Lead Removal by Activated Citrus Sinensis Biochar Impregnated with Calcium Alginate Beads

VANDANA KACHHWAHA, POOJA KUMARI, NARESH GIRI and PALLAVI MISHRA*

Department of Chemistry, J. N. V. University, Jodhpur, India.
*Corresponding author E-mail: pallavianuk@gmail.com

http://dx.doi.org/10.13005/ojc/390615

(Received: October 16, 2023; Accepted: November 17, 2023)

ABSTRACT

This study introduces an innovative method of using activated carbon derived from citrus sinensis peels incorporated into calcium alginate beads to remove lead from synthetic water efficiently. This novel approach demonstrates remarkable effectiveness in addressing lead pollution in water. Established techniques such as SEM and FTIR were employed to characterize the adsorbents created in the laboratories. Batch studies confirmed the lead adsorbed were conducted to evaluate the efficiency of lead removal, with the highest removal efficiencies achieved at pH 6.5 (90.3%), an adsorbent dose of 2 mg (90.3%), a contact time of 50 min (92.3%), and an initial lead solution concentration of 20 ppm (93.2%). The study employed various adsorption models, including Langmuir, Freundlich, and Tempkin models. The Langmuir model exhibited an excellent fit to the adsorption isotherm at 60°C, as indicated by a high linear regression correlation coefficient. For the bioadsorption process, pseudo-second-order kinetics fits well (R^2=0.9992). The analytical results verify that activated carbon from discarded orange peels and calcium alginate beads effectively removes Pb, offering an encouraging solution for water purification challenges.

Keywords: Biosorption, Toxic heavy metal ions, Calcium alginate, Bioadsorbents, Percentage removal efficiencies.

INTRODUCTION

Lead contamination in wastewater and natural water is a significant concern due to its high toxicity to aquatic life, the environment, water quality, and human health. Lead accumulation through the food chain can lead to various human diseases, including cancer, anaemia, paralysis, and lead poisoning. Multiple industries, such as battery manufacturing, dye and pigment production, plastic manufacturing, steel production, electronics, and pesticides, contribute to metal-enriched wastes[1] like lead discharge into the environment, necessitating the treatment of lead-contaminated wastewater before release. Various industries generate lead waste, including textiles, smelting, and battery manufacturing. Lead is a toxic substance[2] that accumulates in different body parts, such as the brain, liver, kidneys, and bones. It poses a significant risk to young children; it builds up in teeth and bones over time. Usually, blood lead levels are used to assess human exposure.[3] During pregnancy, lead stored in bones is released into the bloodstream, exposing the growing fetus.[4,5,6] This exposure to

lead is very harmful to the fetus. Young children are especially at risk from lead's toxic effects, which can severely and permanently impact their health, particularly the developing brain and nervous system.[7,8] Lead exposure in adults can lead to elevated blood pressure and kidney issues.

Bioadsorption[9,10] is proposed as an efficient, cost-effective, and environmentally friendly method for heavy metal removal in wastewater. Adsorption offers a range of adsorbent choices depending on the target ions, budget, and water quality requirements. The bioadsorption process is simple, reversible, economically beneficial, and better than conventional methods. Compared to other physicochemical treatment techniques, adsorbents are economical, eco-friendly, and harmless. This process produces less sludge, and it is simple to operate. Different benefits of the bioadsorption method include cheap operating costs, a small volume of disposable sludge, excellent efficacy in detoxifying very diluted effluents, etc.[11,12] Bioadsorbents are more efficient for heavy metals than other conventional methods (like ion exchange resins) because they have more binding capacity. Bioadsorbents can be regenerated, and the removal process is reversible. Bioadsorbents from agricultural or food industry wastes comprise residues like corn cobs, soybean hulls, cotton seed hulls, and fruit peels that have been reported.[13-19] The cell walls with cellulose material having functional groups like phenols or carboxylic acids can undergo cationic exchange with metal ions.

Citrus sinensis commonly known as sweet orange, mainly contains cellulose, hemicellulose, pectin, lignin, chlorophyll pigments, and other low molecular weight hydrocarbons.[20] These chemical constituents have anionic functional groups on their surface. These functional groups contribute to the negative surface charge. So, these groups can adsorb positively charged heavy metal ions.

Activated carbon is a processed microcrystalline carbon that lacks a graphite structure and contains internal porosity. Due to its considerable porosity, extensive surface area, and robust surface reactivity, activated carbon is a remarkably versatile substance.[21] It possesses a specific surface area, ranging from 450 to 2,000 m²/g, which significantly aids in the biosorption of gases or any soluble matter from liquids.[22] Its numerous minute pores contribute to an expansive inner surface and exceptional adsorption properties. AC effectively captures various water and wastewater pollutants, including organic, inorganic, microbiological, and biological contaminants.[23,24] Charcoal is an amorphous allotrope of carbon. Charcoal can adsorb many substances, including heavy metal ions, because this material has a high porosity, offering a vast surface area for pollutants to adhere to. The charcoal was formed from the orange peel. Alginate, linear non-branched polysaccharides, is derived from brown seaweed. Alginate is known for its ability to create gels in the presence of calcium ions, which makes it useful for thickening, stabilising, and gelling a wide range of heavy metals to some extent.[25] We have used activated charcoal and calcium alginate beads combination for the bioadsorption of lead. Lead from water can be removed using this technology cost-effectively and environmentally friendly. However, laboratory tests are crucial to ascertain the effectiveness of lead removal under specific circumstances.

MATERIALS AND METHODS

Charcoal Preparation

First, the orange peels were carefully collected and washed to remove dust or unwanted particles. Subsequently, the peels were cut into small fragments and dried. Then, we crushed and milled the dried samples. The powder of orange peel was heated at a temperature between 400°C to 800°C for one hour in a muffle furnace using a porcelain crucible to form charcoal, and then it was cooled at room temperature. Sulphuric acid was used to activate the charcoal and to increase its adsorption capacity. Charcoal was mixed with the acid, and then it was left at room temperature overnight. Its modifications were done for heavy metal removal instead of using charcoal directly. We used combinations of charcoal with calcium alginate (CA) in the form of beads to increase the adsorption capacity.

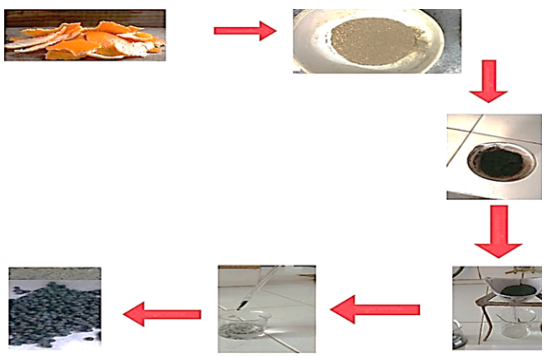

Fig. 1. Acid-treated orange peel charcoal with calcium alginate beads formation

(Orange peel->dried Orange peel powder ->charcoal->acid treatment of charcoal->beads formation process->Beads).

Then 2 mg acid-treated charcoal and 2% sodium alginate solution were mixed, which was added dropwise to 2% calcium chloride solution. Then, acid-treated orange peel charcoal-calcium beads were formed. These beads were introduced to the oven at 50°C for 24 hours. This acid treatment increases the adsorption capacity. These beads were used as adsorbents.

Preparation of lead ion solution

In 50 mL of deionised distilled water, 1.61 g of lead nitrate were dissolved to produce a 1000ppm stock solution of lead. Using a 1000 mL volumetric flask, distilled water was added to bring the volume to one litre.

Preparation of sample solution

10 mL of stock solution was diluted with 90 mL of distilled water. The sample solution was 100 mL of 10ppm concentration.

RESULTS AND DISCUSSION

The study utilised activated carbon (AC) derived from orange peels and CA (calcium alginate) beads combined as adsorbents. The characterisation of this orange peel AC and CA was carried out using various techniques.

Characterisation

We have used characterisation techniques like FTIR and SEM to give a thorough grasp of the physical, chemical, and structural properties of the orange peel AC and CA beads, which is crucial for assessing their suitability as an adsorbent in various applications, such as adsorption of pollutants or chemicals from aqueous solutions.

SEM Analysis

The surface morphology of the OPAC and OPACCAB samples was visualised and examined using scanning electron microscopy (SEM). The treated OPAC and OPACCAB SEM images were obtained using Carl Zeiss EVO MA[25].

Scanning electron microscopy analysis result

Scanning electron microscopy (SEM) effectively observes materials' surface morphology and microstructure at high magnifications. It can analyse the composition of calcium alginate beads and orange peel-activated charcoal.

SEM analysis of treated orange peel charcoal

The treated charcoal was examined for its surface and functional characteristics using the following techniques.

The instrument used for the SEM analysis was Carl Zeiss EVO MA[25].

SEM micrograph of orange peel AC at 1000X(100µm at 20kV) is represented in Fig. 2. Activated orange peel charcoal typically has a rough and porous surface structure, as seen in the SEM image. The activation produces a highly absorbent substance with uneven surfaces and many holes or pores. It indicates that the outside surface of the AC has uniformly open macropores where the dark area resides; after being subjected to carbonisation, orange peel AC develop voids (called pores), responsible for the microporous network.

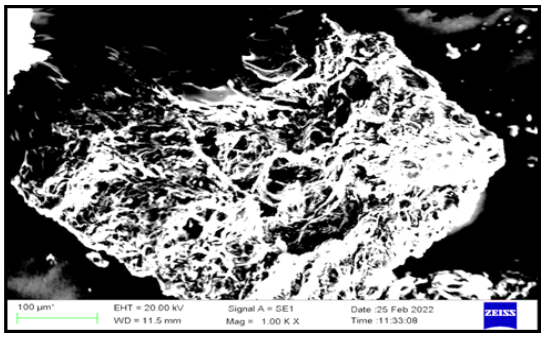

Fig. 2. Micrograph of Treated charcoal at 1000K magnification

SEM analysis of Activated Orange Peel charcoal-calcium alginate beads (AOPCCAB) (Unused)

SEM micrograph of orange peel AC with calcium alginate beads at 2000X(20µm at 20kV) is represented in Figure 3.

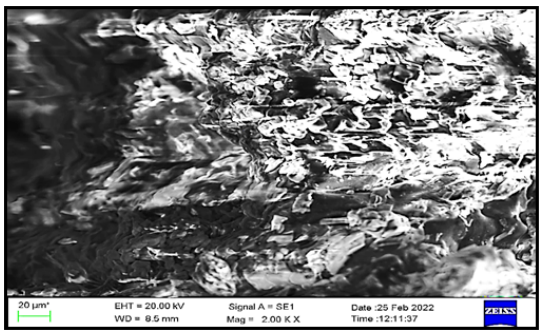

Fig. 3. Micrograph of Un-Used AOPCCAB at 2000k magnification

A distinct structure can be seen in the SEM image of calcium alginate beads infused with activated orange peel charcoal. The beads have a smooth, homogeneous surface texture and a spherical or bead-like appearance. We can see consistent bead sizes in the SEM image; the beads are generally homogeneous in size and shape. The impregnated charcoal preserves its porosity even though the beads are not porous like activated charcoal. We can see that the charcoal flakes inside the beads have a porous structure.

SEM analysis of Activated Orange Peel charcoal-calcium alginate beads (Used)

SEM analysis of treated Orange Peel charcoal-calcium alginate beads (Used) 2000X (20µm at 20kV) is represented in Fig. 4. The image indicates a more uniform structure with filled spaces. The SEM analysis of beads displayed the microstructure at different magnifications. Since there is a weak diffusion resistance force in composite beads, it was supposed that lead adsorption onto alginate beads occurs via two mechanisms: one is through polymeric networks, and the other is through electrostatic interactions available at the adsorbent's porous site, which enables pore diffusion. The magnification of 2000X (20µm at 20kV) exhibits the presence of a polymeric solid network attributed to alginate's polyuronide moieties that chelate with calcium, resulting in a crosslinked polysaccharide chain, which is evident in its microstructure helps in trapping the adsorbate ion. The micrograph represents the polymeric moiety around the cavities or pores. The accumulation of biochar onto the alginate surface was also clearly apparent in the SEM micrograph, making alginate nanocomposites an excellent adsorbent.

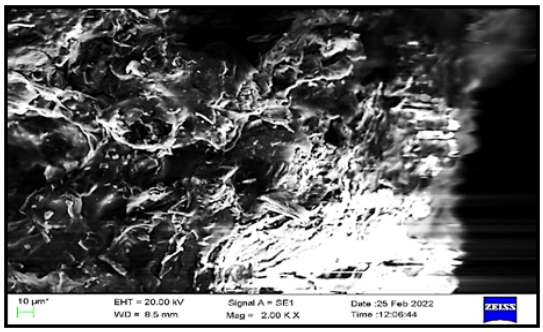

Fig. 4. Micrograph of used AOPCCAB at 2000K magnification

The EDS further confirmed the lead adsorption.

FTIR Spectroscopy: To determine the types of chemical bonds and functional groups present in the orange peel AC and CA beads, Fourier Transform Infrared (FTIR) spectroscopy was performed. FTIR spectra were recorded in the 3500 to 800 cm^{-1} region before and 3500 after sorption. This technique measures the absorption of infrared light by the material.

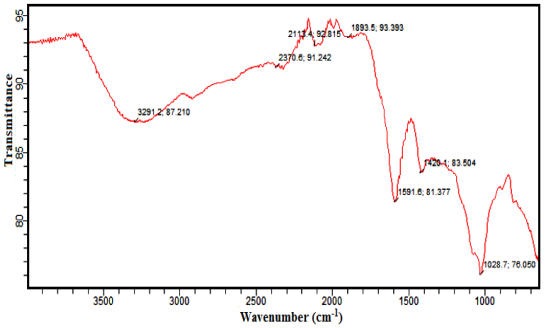

Fig. 5. FTIR of Orange peel-activated carbon before adsorption

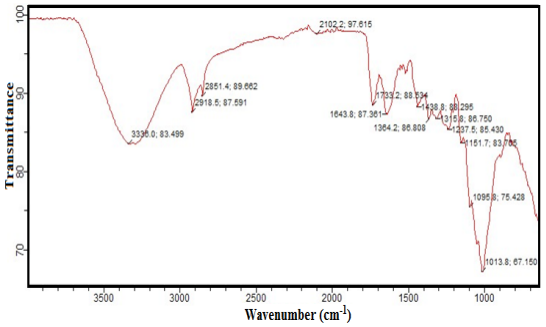

Fig. 6. FTIR of Orange peel-activated carbon after adsorption

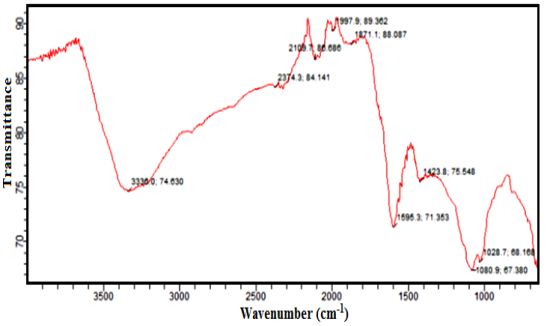

Fig. 7. FTIR of Alginate beads

The FTIR analysis of alginate beads supports calcium alginate structure and activated charcoal's

presence. These characterisation techniques comprehensively understand the orange peel AC's physical, chemical, and structural properties. This is crucial for assessing its suitability as an adsorbent in various applications, such as the adsorption of pollutants or chemicals from aqueous solutions.

Bioadsorption process

The process involves mixing the bio-adsorbent (acid-treated orange peel charcoal with calcium alginate beads) with a lead-containing sample solution for a specific duration. During this time, the biosorption of lead ions occurs on the surface of the bioadsorbent, depending on the adsorption kinetics. Once equilibrium is reached, the bioadsorbent is separated from the metal ion solution using filtration. The lead metal ion solutions are then analysed using AAS.[26] These experiments were conducted in our laboratory, and the samples were analysed at PCB Jodhpur. Heavy metal-containing water affects soil fertility and cause health hazards.[27] The Heavy hazardous metals cannot be destroyed chemically. Physical methods should be used to remove them.[28] So, we used the biosorption method.

The percentage removal of lead was calculated using a specific formula.

% removal efficiency (%RE) = Co- Ce × 100/ Co

Where Co=initial concentration of lead solution in ppm

Ce=residual concentration of the lead solution in ppm

We studied the factors influencing the removal of lead metal ions using acid-treated Orange peel charcoal immobilised in calcium alginate beads. We investigated the impact of pH, dose of bio-adsorbent, contact time, temperature, and initial lead ion concentration in the solution.

Effect of pH

The pH variation was carried out over a pH range from 3.5 to 8.0. We used 0.1M HCl or 0.1M NaOH for adjustment of pH. Due to the strong electrostatic interactions between adsorbate (lead metal ions)-adsorbent, they show high adsorption capacity at lower pH. The maximum removal efficiency was attained at pH 6.5 (90.3%).

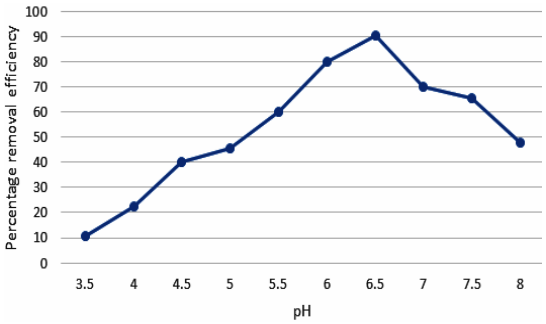

Fig. 8. Effect of pH on bioadsorption of Lead

Effect of bio adsorbent dose

The amount of adsorbent used is crucial as it influences the capacity for bioadsorption at a given initial concentration. When the bio-adsorbent dose increases, the bioadsorption rate increases due to the larger surface area available. However, an excessive concentration of bioadsorbent can lead to the aggregation of adsorbed ions on the biomass surface, reducing the number of active sites and potentially hindering the adsorption process.

In our study, we analysed the removal of lead ions by increasing the acid-treated orange peel charcoal with calcium alginate beads dose. Bioadsorption increases with increasing the dose of bioadsorbent. We have increased the dose of bio adsorbent from 0.5 mg to 3 mg and then studied the change in percentage removal efficiencies. Maximum removal efficiency of 90.3% was obtained at a 2 mg dose.

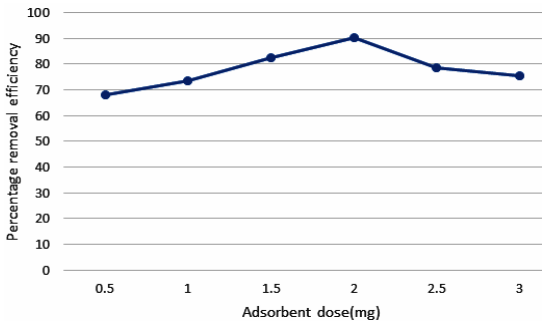

Fig. 9. Effect of bio adsorbent dose on bioadsorption of Lead

Effect of contact time

There are two stages for Pb ion removal. Lead ions are quickly removed in the first stage because more active sites are available. But most functional sites are filled with metal ions after some

time, so a prolonged removal process occurs in the second stage. The graph shows that the maximum removal efficiency of 92.3% was obtained at 50 min of contact time. The removal rate increased initially very fast, but after some time, a prolonged removal process took place, and finally, it became almost constant.

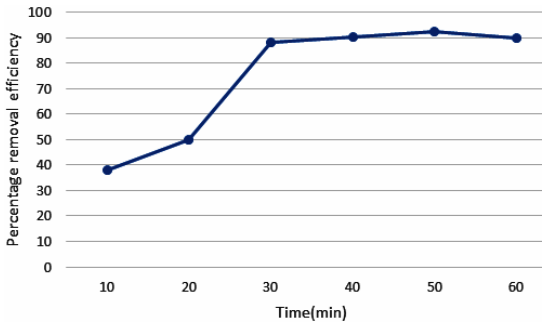

Fig. 10. Effect of contact time on bioadsorption of Lead

Effect of initial concentration of the lead solution

Lead ions are effectively adsorbed at low initial metal ion concentrations because more active sites are available. Still, at higher initial metal ion concentrations, the removal process becomes slow due to less availability of active sites. Maximum lead ion removal efficiency was obtained at 20 ppm (93.2%) lead ion solution concentration. The following graph shows that minimum lead ion removal efficiency was obtained at 120 ppm (51.2%).

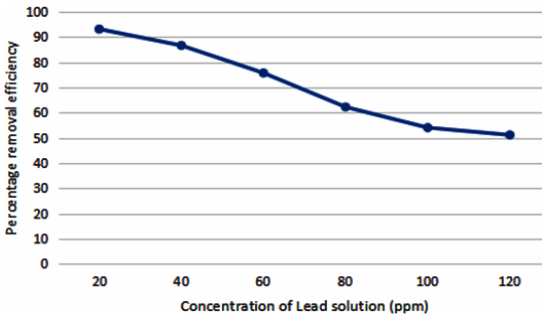

Fig. 11. Effect of initial concentration of lead on bioadsorption of lead

Effect of temperature

The effect of temperature on lead ion removal was analysed at temperatures like10°C,20°C,30°C,40°C,50°C and 60°C. The following graph shows the percentage removal efficiency with an increase in temperature. It is clearly shown in the graph that maximum removal efficiency (82.3%) was obtained at room temperature (30°C). After this removal, efficiency decreases with an increase in temperature.

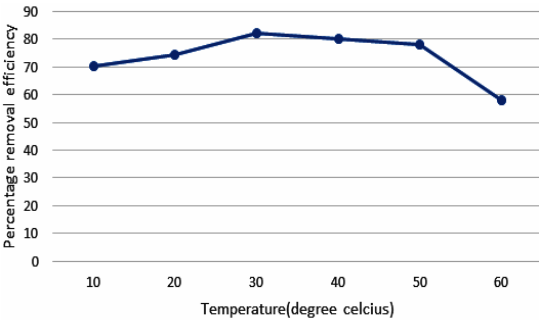

Fig. 12. Effect of temperature on bioadsorption of lead

Isotherm study

We studied Freundlich, Langmuir and Tempkin isotherm models for the bioadsorption process.

Freundlich Isotherm

Generally represented as

$q=x/m = KfCe^{1/n}$

Linear form

$$\log(q_e)=\log x/m=\log(K_f)+1/n \log(C_e) \quad (1)$$

Where q_e=the x amount of metal ions adsorbed on mass m of the adsorbent at pressure P at equilibrium (q_e=x/m) (mg adsorbate/g adsorbent) K_f=Freundlich constant, which shows adsorption capacity (l/g)

1/n=Adsorption intensity

V=volume of the aqueous phase (mL)

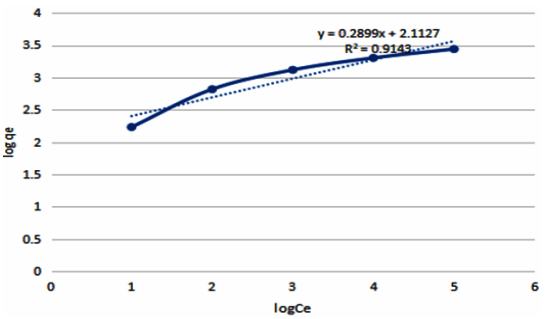

Fig. 13. Freundlich adsorption isotherm for lead removal

The log x/m (q_e) against the log C_e plot was a straight line shown in the graph. From the plot's intercept (log K_f), the Freundlich constant K_f was calculated, which was 8.27. From the slope (1/n)

of the plot, adsorption intensity 1/n was obtained, which was 0.2899. The regression coefficient R2 was 0.9143 for Freundlich isotherm.

Langmuir Isotherm

Generally represented as

$q_e = qmax b C_e/(1+bC_e)$ (Nonlinear form)

$C_e/q_e = 1/b\ qmax + C_e/qmax$ (Linear form),

When a graph was plotted between C_e/q_e and C_e, it gave a straight line. This indicates the applicability of Langmuir isotherm.

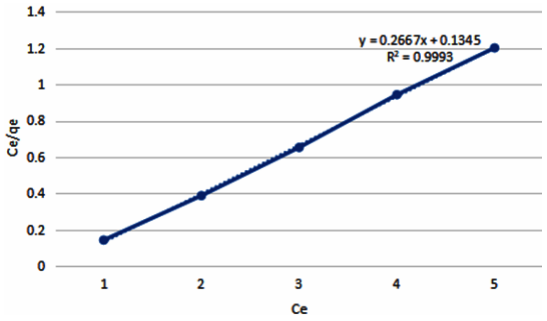

Fig. 14. Langmuir adsorption isotherm for lead removal

The Langmuir constant b and the qmax value were determined from the slope (1/qmax) and intercept (1/bqmax) with the y-axis. The qmax value was 3.7495, and the Langmuir constant value b was 1.98. The regression coefficient R2 for Langmuir isotherm was 0.9993.

Tempkin Isotherm

Generally represented as

$q_e = a + 2.303\ b \log C_e$

q_e against log C_e, the plot can be used to calculate isotherm constants a and b from the slope and the intercept.

q_e against log C_e, the plot gives the values of isotherm constants a,b from the intercept (a) and slope(2.303b). The Tempkin parameters a and b values were 5.139 and 2.3569, respectively. The Regression coefficient value was 0.9843 for Tempkin isotherm.

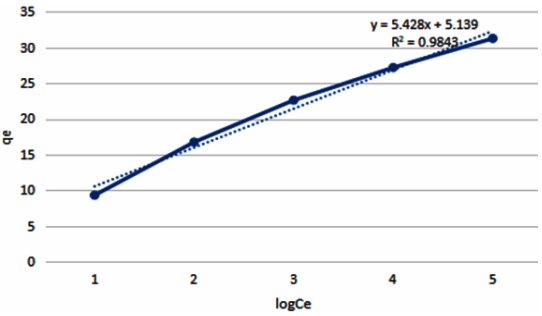

Fig. 15. Tempkin adsorption isotherm for lead removal

Table 1: Comparison of Freundlich, Langmuir and Tempkin constants for Pb bioadsorption by acid-treated Orange peel charcoal with calcium alginate beads

Metal	Freundlich			Langmuir			Tempkin		
	Kf	1/n	R2	Qm	b	R2	a	B	R2
Pb	8.27	0.2899	0.9143	3.7495	1.98	0.9993	5.139	2.3569	0.9843

Freundlich, Langmuir and Tempkin isotherms for Pb ions bioadsorption were linear, as shown in their graphs. It shows the applicability of the isotherms.

Based on regression coefficient values, the applicability of isotherm models for our present study follows the order of Langmuir>Tempkin>Freundlich. It shows that kinetics for lead removal by acid-treated orange peel charcoal with calcium alginate beads fitted well in the Langmuir adsorption isotherm.

Adsorption Kinetics

Pseudo-first order was not applicable for lead bioadsorption by Orange peel charcoal with calcium alginate beads.

So, we have done the kinetic study for pseudo-second-order, which was carried out at pH 6.5 Using linear regression plots, the kinetics modelling was tested.

Table 2: Time and t/qt values

Time(min)	t/qt
10	1.0723
20	1.1940
30	1.3268
40	1.4716
50	1.6

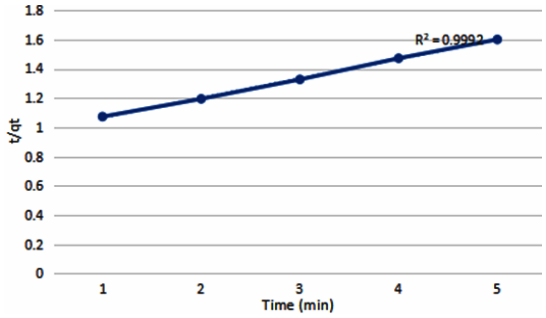

Fig. 16. Pseudo-second-order kinetic model plot for Pb bioadsorption

A graph was plotted between time in minutes and t/qt based on linear regression (R2>0.99). The kinetics of Pb bioadsorption by acid-treated orange peel charcoal-calcium alginate beads can be described well by pseudo-second-order with a 0.9992 value of R2. The results show that this study fits well with pseudo-second-order kinetics.

CONCLUSION

This study demonstrates that acid-treated orange peel charcoal-calcium alginate beads are highly effective in removing lead ions from synthetic wastewater, thereby mitigating lead pollution in water. Among the tested materials, the acid-treated orange peel charcoal with calcium alginate beads exhibited the highest efficiency in lead removal and is a promising alternativefor treating industrial waste containing lead ions. Characterisation of these beads through techniques like FTIR and SEM revealed a substantial surface area suitable for bioadsorption. Additionally, this bioadsorbent is readily available and cost-effective, making it a more economical choice than other bioadsorbents. The adsorption of lead metal ions onto the acid-treated orange peel charcoal with calcium alginate beads reached equilibrium within just one hour, achieving a remarkable removal efficiency of 93.2%. Analysing the data, we found that the adsorption isotherm models best fit the Langmuir model, followed by the Tempkin and Freundlich models. Given their cost-effectiveness, orange peel charcoal and calcium alginate beads emerge as an attractive option for communities and organisations grappling with budget constraints related to water treatment and environmental cleanup projects.

ACKNOWLEDGEMENT

We thank the Pollution Control Board and Defense Laboratory in Jodhpur for granting us access to the necessary instrument facilities for conducting our experiments. We also thank the Department of Chemistry at JNVU, Jodhpur, for their valuable support.

Conflict of interest

The authors declare no conflict of interest in the present work.

REFERENCES

1. Nriagu, I.O. *Global Metal Pollution. Environment.*, **1990**, *32*, 7-33.
2. Gulson, B. L.;Taylor, A. J. The toxicology of lead in adults. *In Handbook on the Toxicology of Metals (Fourth Edition),* **2017**, 385-435.
3. Preventing disease through healthy environments: exposure to lead: a primary public health concern. *World Health Organization.,* **2019**.
4. Silbergeld, E.K. (1991). Lead in bone: implications for toxicology during pregnancy and lactation. *Environmental health perspectives.*, **1991**, *91*, 63-70.
5. Needleman,H. Lead poisoning. *Annu Rev Med.*, **2004**, *55*, 209-222.
6. ATSDR. Toxicological Profile for lead. Agency for Toxic Substances and Disease Registry., **2007**.
7. Sanders, T.; Liu, Y.; Buchner, V.; Tchounwou, P.B. Neurotoxic effects and biomarkers of lead exposure: a review. *Reviews on Environmental Health.*, **2009**, *24*(1), 15-46.
8. WHO. Childhood Lead Poisoning. World Health Organization., **2010**.
9. Shamim, S. Comparative analysis of metal resistance, accumulation, and antioxidant enzymes in Cupriavidus metallodrugs CH_{34} and Pseudomonas putida mt2 during cadmium stress. Ph. D. thesis. Department of Microbiology and Molecular Genetics, University of the Punjab: Pakistan., **2016**.
10. Fulekar, M.H.; Singh, A.; Bhaduri, A.M. Genetic engineering strategies for enhancing phytoremediation of heavy metals. *African Journal of Biotechnology.*, **2009**, *8*(4), 529-535.

11. Choudhary, S.; Sar, P. Characterisation of a metal-resistant Pseudomonas sp. isolated from uranium mine for its potential in heavy metal (Ni^{2+}, Co^{2+}, Cu^{2+}, and Cd^{2+}) sequestration. *Bioresource Technology*., **2009**, *100*, 2482-2492.
12. Sinha, S.; Mukherjee, S.K. Pseudomonas aeruginosa KUCD1, a possible candidate for cadmium bioremediation. *Brazilian Journal of Microbiology*., **2009**, *40*, 655-662.
13. Norberg, A.; Persson, H. Accumulation of heavy metal ions by Zoogloea ramigera. *Biotechnology and Bioengineering*., **1984**, *26*, 239-245.
14. Wang, J. L.; Chen, C. Biosorbents for heavy metals removal and their future-a review. *Biotechnology Advances*., **2009**, *27*, 195-226.
15. Kuyicak, N.; Volesky, B. Biosorption by fungal biomass. In: Volesky, B., editor. Biosorption of Heavy Metals. Florida: CRC press. **1990**, 173-198.
16. Khani, M.H. Uranium biosorption by Padina sp. algae biomass: Kinetics and thermodynamics. *Environmental Science and Pollution Research International*., **2011**, *18*, 1593-1605.
17. Flouty, R.; Estephane, G. Bioaccumulation and biosorption of copper and lead by a unicellular algae Chlamydomonas reinhardtii in single and binary metal systems: A comparative study. *Journal of Environmental Management*., **2012,** *111*, 106-114.
18. Trinelli, M.A.; Areco, M.M.; Mdos, S.A. Co-biosorption of copper and glyphosate by Ulva lactuca. *Colloids and Surfaces B: Biointerfaces*., **2013**, *105*, 251-258.
19. Kelly-Vargas, K.; Cerro-Lopez, M.; Reyna-Tellez, S.; Bandala, E.R.; Sanchez-Salas, J.L. Biosorption of heavy metals in polluted water, using different waste fruit cortex. *Physics and Chemistry of the Earth*., **2012**, *37-39*, 26-29.
20. Liang, L.P.; Wang, Q.; Xi,F.F.; Tan, W.S.; Zhang, Y.T.; Cheng, L.B.; Wu, Q.; Xue, Y.Y.; Meng,X. Effective Removal of Cr (VI) from Aqueous Solution Using Modified Orange Peel Powder: Equilibrium and Kinetic Study. *Nature Environment & Pollution Technology*., **2020**, *19*(4), 1391-1398.
21. Bokil, S. A.; Rai, R. K. Preparation and characterisation of activated carbon from bamboo by chemical activation. *Journal of Catalyst and Catalysis*., **2016**, *3*(1), 1–6.
22. Hameed, B. H.; Din, A. T. M.; Ahmad, A. L. Adsorption of methylene blue onto bamboo-based activated carbon: kinetics and equilibrium studies. *Journal of Hazardous Materials*., **2007**, *141*, 819–825.
23. Akar, S. T.; Ozcan, S.; Akar, T.; Ozcan, A.; Kaynak, Z. Biosorption of a reactive textile dye from aqueous solutions utilising an agro waste. *Desalination*., **2009**, *249*(2), 757-761.
24. Balci, B.; Keskinkan, O.; Avci, M.Use of BDST and an ANN model for prediction of dye adsorption efficiency of Eucalyptus camaldulensis barks in fixed-bed system. *Expert Systems with Applications*., **2011**, *38*(1), 949–956.
25. Oyedepo, T.A. Biosorption of lead (II) and copper (II) metal ions on Calotropis procera (Ait.). *Science Journal of Pure and Applied Chemistry*., **2011**, *1*, 1-7.
26. Mishra, P.; Soni, R.; Kachhwaha, V.; Giri, N. Assessment of toxic metals in common food grains grown in Jodhpur city. *Rasayan J. of Chem*., **2020**, *13*(1), 210-214.
27. Kachhwaha, V.; Sharma, G.; Tanwar, P.; Mishra, P. Using Multivariate Statistics to assess Water Quality Indices of Heavy Metal Pollution in Jojari River (Jodhpur). *Eco. Env. & Cons*., **2022**, *28* (August Suppl. Issue), S301-S310.
28. Kachhwaha, V.; Mishra, P. Assessment of Heavy Metal Pollution Index (HPI) In The Vegetables Collected From The Local Markets, Fields and Beras in Jodhpur City. Rajasthan (India). *Bull. Env. Pharmacol. Life Sci.* **2022**, Spl Issue [1], 1096-1101.